Uranium Dynamic Adsorption Breakthrough Curve onto Rice Straw Based Activated Carbon Using Bed Depth Service Time Model

Sobhy Mostafa Ebrahim Yakout,[a,b,*] Ahmed Abdelsattar Abdeltawab,[c] Khalid Elhindi,[d] and Ahmed Askalany [e]

Uranium adsorption was evaluated on rice straw-based carbon (RSK carbon) that had been KOH-oxidized and impregnated with ionic-liquid. Experiments were performed in fixed bed mode using 100 mg/L uranium solution at 3 different bed depths (12, 6, and 3 cm). Uranium adsorption decreased with increasing bed depth. Agreement between column and batch values was judged to be acceptable in light of inherent differences in continuous *versus* batch operations. Batch mode reaches equilibrium without continuous solution feeding. However, the solution in fixed bed mode was fed constantly without equilibrium. The bed depth service time (BDST) model was used to investigate uranium adsorption. BDST plots were linear, with a high correlation coefficient ($R > 0.97$), representing its validity when used for fixed bed of RSK carbon. The failure of the 50% breakthrough BDST curve to pass through the origin point may be due to the complex mechanism of uranium removal by RSK carbon. The calculated BDST slopes were in good agreement with the experimental values, while the values of their intercept slightly varied within certain limit of experimental error. These results support the validity of BDST model for designing a fixed bed column for uranium adsorption onto RSK carbon.

Keywords: Breakthrough curve; Fixed-bed column; Activated carbon; Uranium adsorption; BDST model

*Contact information: a: Biochemistry Department, College of Science, King Saud University, PO Box 2455, Riyadh, 11451, Kingdom of Saudi Arabia; b: Atomic Energy Authority, Hot Laboratories Centre, 13759, Egypt; c: Chemistry Department, College of Science, King Saud University, Riyadh 11451, Saudi Arabia; d: Plant Production Department, College of Food and Agriculture Sciences, King Saud University, P.O. Box 2460, Riyadh 11451, Saudi Arabia; e: Mechanical Engineering Dept., Faculty of Industrial Education, Sohag University, Sohag 82524, Egypt; *Corresponding author: syakout@ksu.edu.sa*

INTRODUCTION

Adsorption in solution takes place through batch and column modes (Xu *et al*. 2013). Column mode is favored in extensive applications of water treatment because of its easy operation and flexibility (Rojas-Mayorga *et al*. 2015). An adsorption column is well known to show non-linear behavior that can be investigated by breakthrough curves. Water or wastewater is introduced to the carbon column, and effluent contaminant concentration is monitored *versus* the volume of liquid treated (or time). Initially, adsorption takes place at the top of the column in a narrow band, called the adsorption zone or mass transfer zone (MTZ) (Faust and Aly 1983). As the operation continues, the top layer of the activated carbon become saturated (dark shading) with solute and MTZ (light shading) progress downward through the bed as shown in Fig. 1. Eventually, the MTZ reaches the bottom of the column, and the adsorbant level in the effluent starts to rise. Plotting the concentration

of the effluent solution against its treated volume (or time) produces an S-shaped curve ("breakthrough" curve) that is a function of sorber geometry, as well as operating conditions and equilibrium data. The breakthrough point on the curve indicates where the adsorbate reaches its maximum permissible concentration. The exhaustion point occurs where the adsorbate concentration reaches 95% of its inlet concentration (Hussin 2003). A typical breakthrough curve is shown in Fig. 1 (USACE 2001). The breakthrough time is the point where the outlet concentration reaches 5% of the inlet concentration ($C_t = 0.05C_o$), and the exhaustion time occurs when $C_t = 0.95C_o$ (Chern and Chien 2002). The breakthrough time and breakthrough curve shape are important features for measuring the operation and dynamic response of fixed-bed adsorption column. The overall breakthrough curve position along the volume or time axis is based on column capacity with respect to i) inlet adsorbate concentration, ii) solution flow-rate, and iii) column bed-depth.

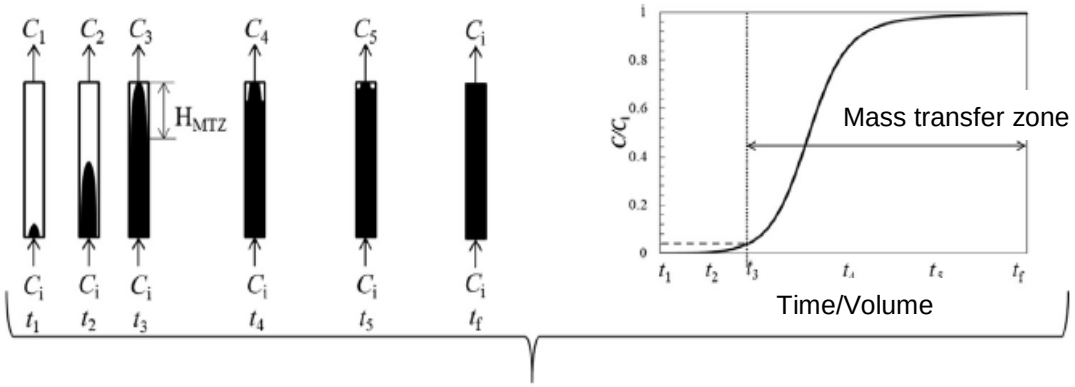

Fig. 1. Breakthrough curve in column operation (USACE 2001)

Previous work described uranium removal by rice straw carbon in batch mode (Yakout *et al*. 2013; Yakout 2015; Yakout *et al*. 2015; Salema and Yakootb 2017). Batch mode offers significant information on carbon efficiency to remove uranium such as equilibrium time, concentration, carbon dose, and pH for maximum uranium adsorption. As an extension of previous work, this study used KOH-oxidized and rice straw-based carbon (RSK carbon) for the uranium removal in fixed-bed column with different bed depth. The breakthrough curves were analyzed to associate uranium uploading and its elution volume and time. Breakthrough curves were studied using bed depth service time (BDST) model to calculate column capacity and predict its performance along with some other process parameters required in design and scale-up results to other systems.

Present study results will be of considerable importance in optimization of a dynamic adsorption processes for radioactive elements removal from aqueous solution by justification of dynamic adsorption processes and bed configuration.

EXPERIMENTAL

Preparation and Characterization of Activated Carbon

KOH-oxidized and rice straw-based carbon (RSK carbon) was prepared using the reported method in earlier papers (Yakout *et al*. 2013; Yakout 2015; Yakout *et al*. 2015; Salema and Yakootb 2017). Activated carbon was impregnated by ionic liquid according

to previously published procedure (Ismaiel *et al*. 2013). Actually, treatment of RSK carbon with ionic liquid has no significant influence on the adsorption of uranium. Therefore RSK carbon was used without ionic liquid modification in the rest of study.

All physicochemical characteristics, *e.g*., Fourier-transform infrared spectroscopy (FTIR), porosity, and scanning electron microscope (SEM) images of RSK carbon were previously reported (Yakout *et al*. 2013; Yakout 2015; Yakout *et al*. 2015). The influence of RSK porosity and surface chemistry on uranium (VI) removal was also discussed in a recent article (Yakout 2016).

Column studies

As shown in Fig. 2, known amounts of RSK carbon were added to glass column (i.d. 0.8 cm) using slurry method (ASTM D6586-00 2000) to exclude air bubbles that decrease bed performance. Three runs at different 3-bed depths (3 cm, 6 cm, and 12 cm) were conducted at 100 mg/l uranium initial concentration and 3 mL/min of solution flowrate by means of a peristaltic pump (Milton Roy model Type 131A, Pennsylvania, U, USA). Uranium was prepared from uranyl nitrate (BDH, Poole, England). A fraction collector (spectra/Chrom CF-1, Spectrum Laboratories Inc., California, USA) was used to collect effluent samples, and uranium concentration was measured using a coloring agent (arsenazo III, Sigma-Aldrich, Steinheim, Germany). The spectrum was recorded by using UV-1700 Shimadzu (Shimadzu Co., Japan) UV–Visible spectrophotometer (Marczenko 1986).

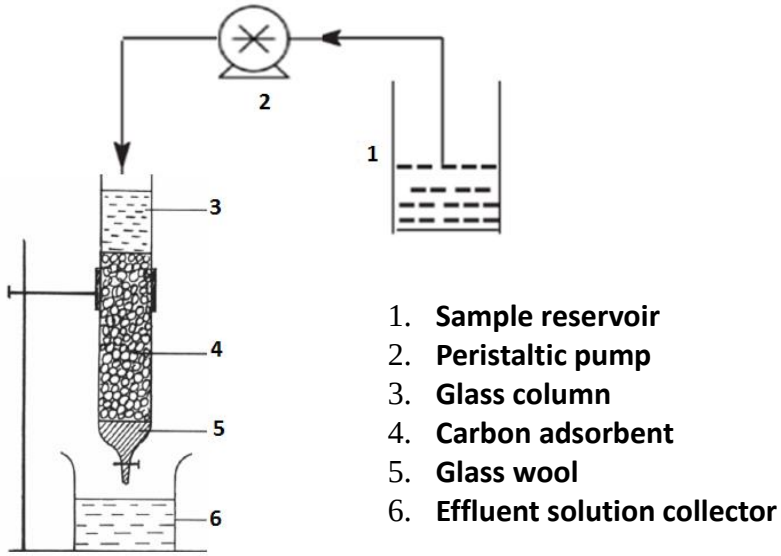

Fig. 2. Column experiment operation

RESULTS AND DISCUSSION

Batch Adsorption Parameters

Batch adsorption parameters must be specified in order to study the dynamics of a fixed bed. Uranium batch adsorption has been discussed in previous publications (Yakout *et al*. 2013; Yakout and Rizk 2015; Yakout 2016). A pH of 5.5 and equilibrium time of 1 h were chosen as the optimum conditions for uranium removal by RSK carbon. The Langmuir and Freundlich parameters are given in Table 1.

Table 1. Freundlich and Langmuir Parameters of Uranium Adsorption onto RSK Carbon (Yakout *et al.* 2013; Yakout and Rizk 2015; Yakout 2016)

Model	Parameter	Value
Freundlich	*K* (mg/g)	33.7
	n	3.5
	R^2	0.9
Langmuir	q^o (mg/g)	100
	b (1/mg)	0.28
	R^2	0.999

Effect of Bed Depth on Uranium Breakthrough Curve

Operational investigations are important for industrial scale-up of adsorber systems for essential applications and performances. This could be achieved by changing adsorber characteristics during the column experiments, thus enabling the prediction of removal performance in a full-scale system. The influence of bed height on uranium sorption behavior were presented and discussed.

Uranium adsorption at different bed depths (12, 6, and 3 cm) was performed. Column parameters are given in Table 2, and breakthrough plots are shown in Fig. 3. With increasing column depth (carbon amount), the breakthrough curve slope decreased and service time increased. At bed depths of 3, 6, 12 cm, the breakthrough time values (t_b) were 58.3, 130, and 260 min, respectively, with corresponding treated volumes of 175, 390, and 780 mL, respectively. Adsorption capacities were found as 84.5, 77.8, and 76.5 mg/g for the bed depth 3, 6, and 12 cm, respectively, with an average value (q_b) of 79.6 mg/g. Increasing bed depth by increasing carbon amount increases adsorption sites numbers. So longer bed depth take more time to be saturated at constant conditions of uranium concentration and solution flowrate (Tan *et al*. 1996). However, increasing bed depth, increases residence time of solution in the column, let adsorbate molecules to diffuse more in the adsorbent (Yakout 2016).

There have been few comparative studies between batch and fixed bed modes, but there have been many studies of each mode separately. The results in Tables 1 and 2 show that the exhaustion adsorption capacity was higher than in batch mode; however, breakthrough adsorption capacity was low. At the breakthrough point, the contact time was not sufficiently long for the attainment of equilibrium, and therefore, the obtained adsorption capacity was lower than that obtained in batch mode. In contrast, the exhaustion adsorption capacity was higher than that was obtained in batch mode (100 mg/g). Increasing residence time in the column allowed metal ions to diffuse deeper into the adsorbent, which saturated the bed. Furthermore, the solution the in column was always retained fresh at constant concentration, which was expected to produce a high concentration difference between the metal ions on the sorbent and that in the solution. A high concentration difference provides a high driving force for the adsorption process and this may explain why higher adsorption capacities were achieved at exhaustion

The batch (q_b) and fixed bed adsorption capacities (q_{fb}) for the removal of several metal ions on different types of adsorbents are compared in Table 3. Commonly, the adsorption capacity in column mode is less than that in batch mode, but the data in Table 3 reveal that the capacity of fixed bed process sometimes exceeded that of batch processes.

This difference could be due to the following reasons: (i) differences in experimental conditions between batch and column such as contact type between sorbent and metal ions and sorbent/solution ratio (Hemming *et al*. 1997; Chang and Wang 2002);

(ii) differences in adsorption kinetics between batch and column (Allen *et al*. 1995); (iii) differences in the homogeneity of packed carbon substance, and particle spacing (Wise 1993); (iv) loss of sorbent particles through the end of the column, leading to some variations in flow or presence of immovable water zones (Porro *et al*. 2000); (v) the inlet solution in column is constantly pumped, thus metal ions are continuously exchanged until equilibrium that takes place when the outlet metal concentration is equal to the influent one; and (vi) the column equilibrium conditions were greatly affected by solution pH, the effect of which cannot be corrected through the experiment.

Table 2. Column Parameters of Uranium at Different Bed-Depths (*L*)

Process Parameters	*L* (cm)		
	3	6	12
Breakthrough			
V_b (mL)	175	390	780
t_b (min)	58.3	130	260
q_b (mg/g)	84.5	77.8	76.5
Exhaustion			
V_E (mL)	723	930	1530
t_E (min)	241	310	510
q_E (mg/g)	349.3	185.6	150

Note: C_o = 100, Q = 3 mL/min

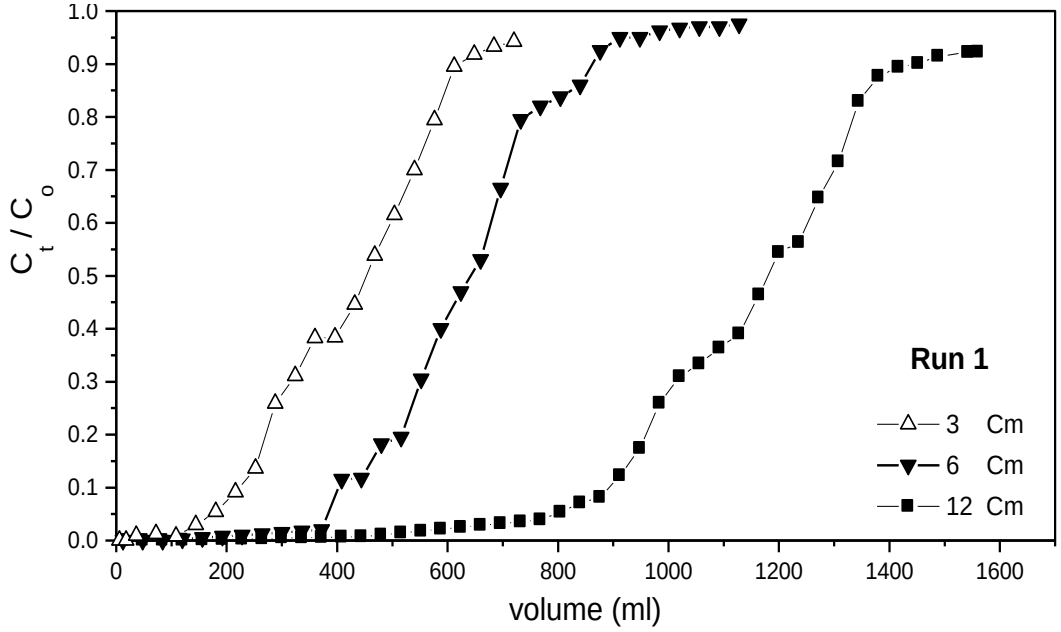

Fig. 3. Experimental breakthrough curves of uranium at different bed depths (3, 6, 12 cm) with respect to volume treated (mL) conditions: C_0= 100 mg/L and Q= 3 mL/min

Table 3. Comparison of the Batch and Fixed Bed Adsorption Capacity for Metal Ions Removal on Different Adsorbents

Adsorbent	Metal Ion	q_b (mg/g)	q_{fb} (mg/g)	Reference
Natural hemp fibers	Co(II)	3.3	12.5	Tofan *et al*. (2013)
		5.8	15.4	
Boron waste	Cd(II)	122.2	138.05	Atar *et al*. (2012)
	Zn(II)	107.7	110.27	
Seaweeds	Co(II)	20.6	50.7	Vijayaraghavan *et al*. (2005)
	Ni(II)	18.6	39.7	
Clinoptilolite-rich tuffs	Cs+	140.6	64.6	Cortés-Martínez *et al*. (2010)
		104.3	46.8	
Zeolite A	Cs+	37.3	32.5	El-Kamash (2008)
		95.6	33.8	
	Sr(II)	44.8	44.5	
		131.2	53.5	
Wheat straw	Cd(II)	14.1	16.9	Muhamad *et al*. (2010)
Mesoporous silica	Pb(II)	52.3	27.6	Shahbazi *et al*. (2011)
		92.2	16.1	
	Cu(II)	52.5	22.2	
		92	12.3	
	Cd(II)	51.3	20.7	
		75.2	9.3	
Polypyrole-graphene oxide	Cr(VI)	138	576	Setshedi *et al*. (2015)
		157	585	
Protonated raw peels	Cd(II)	31	13	Chatterjee and Schiewer (2014)
Protonated alginate peels		43	28	
Fe_3O_4-graphene oxide	Sb(III)	2	3.6	Yang *et al*. (2015)
Alginate	Cr(VI)	431.6	478.62	Yan *et al*. (2017)

Breakthrough Curve Modeling Using BDST Model

A successful adsorber design requires estimation of either a concentration–time profile or breakthrough curves for the adsorbate effluent. Several equations have been used to describe breakthrough curves for industrial applications. Among these equations, the BDST model, which is among the most widely used models, was derived from the Bohart-Adams equation (Bohart and Adams 1920).

The Bohart-Adams model describes adsorption of heavy metal in a fixed-bed column. It is an easy model able to predict the association between bed depth and service time with regard to metal concentration and sorption parameters. This model is useful for estimation of bed characteristics of parameters, such as maximum adsorption capacity. This model is described by the following equation, which suggests an association between bed depth L and service time taken to breakthrough to take place.

$$\ln\left(\frac{C_0}{C_b} - 1\right) = \ln(e^{K_a N_o Z / U} - 1) - K_a C_o t \quad (1)$$

Hutchins (1973) proposed a linear relationship given by Eq. 2,

$$t_b = \frac{N_o}{uC_o} L - \frac{1}{k_a C_o} \ln\left(\frac{C_o}{C_b} - 1\right) \quad (2)$$

where C_o is the initial liquid phase concentration (mg/L); C_b is the effluent concentration at required breakthrough (mg/L); t_b is the service time at required breakthrough (min); N_o is the adsorption capacity (mg/cm^3); L is the bed depth (cm); u is the linear flow rate (cm/min); and K_a is the adsorption rate constant (L/mg. min).

The simplified form of the BDST model is shown in Eq. 3,

$$t_b = m_x - C_x \quad (3)$$

where

$$m_x = \frac{N_o}{C_o u} \quad (4)$$

$$C_x = \frac{1}{k_a C_o} \ln\left(\frac{C_o}{C_b} - 1\right) \quad (5)$$

Bed adsorption capacity, N_o, and the flowrate constant, K_a, can be estimated from the intercept and slope in the plot of t_b *vs*. L, which yields a straight line of slope m_x and intercept C_x. In the BDST equation when t = o, the critical bed depth L_o is given by Eq. 6,

$$L_o = \frac{u}{k_a N_o} \ln\left(\frac{C_o}{C_b} - 1\right) \quad (6)$$

The critical bed depth represents the minimum depth of sorbent needed to produce an effluent sorbate concentration C_b. The BDST model for the sorption of uranium to RSK carbon up to 50% breakthrough (5, 10, 20, 30, 40, 50%) is shown in Fig. 4, and the BDST parameters (K_a, N_o, and L_o) are presented in Table 4. The BDST plots were linear with high correlation coefficient (R > 0.97), signifying that the BDST model is valid for the RSK carbon fixed bed (Zulfadhly *et al*. 2001). As indicted in Table 4 (for 5 and 10 % breakthrough), the critical bed depth, L_o, was lower than 10% of total bed height. This means that the columns under investigation worked well, supporting BDST scale up to the pilot scale (Walker and Weatherley 2001).

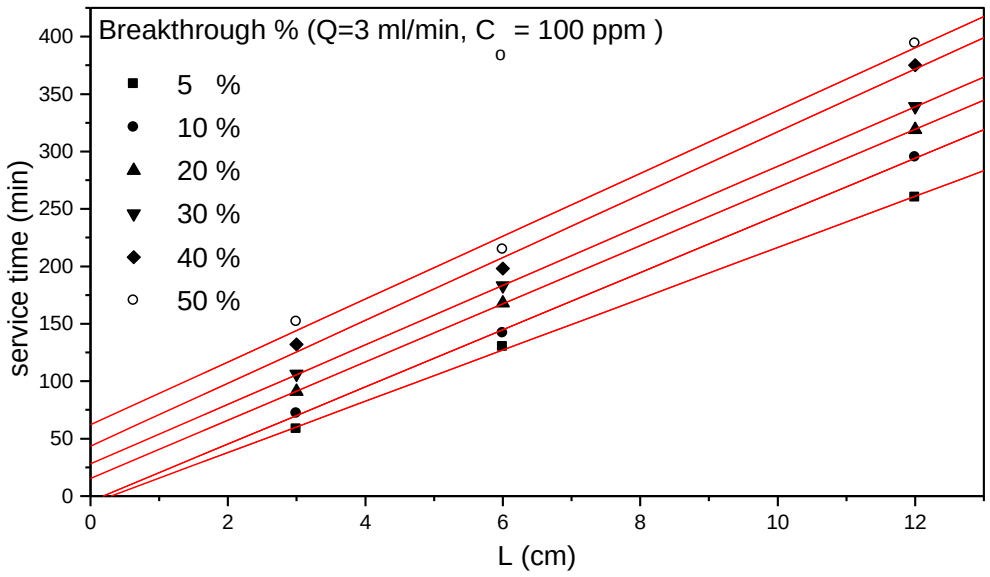

Fig. 4. Effect of breakthrough by BDST model for uranium sorption using RSK carbon

Table 4. The BDST Parameters (N_o, K_a, and L_o) of Uranium Adsorption Column

Breakthrough %	$(N_o)_{exp}$ mg cm^{-3} x 10^2	N_o mg L^{-1}	Isotherm q_e mg g^{-1}	L_o cm	K_a mL. mg^{-1} min^{-1}
5	133.83	78.7	55	0.3	4.4 x 10^{-3}
10	148.49	87.35	75	0.18	4.9 x 10^{-3}
20	151.80	89.3	85	-*	-
30	155.40	91.4	86.5	-	-
40	164.14	96.55	87.5	-	-
50	164.05	96.50	88	-	-

Note: * L_o and K_a could not be calculated due to positive intercept on the BDST plot.

According Table 4, the adsorption capacity N_o value obtained in this study (1.3 to 1.6 mg cm^{-3}) is higher than other previously reported low-cost adsorbents such as grapefruit peel (0.03 to 0.05 mg cm^{-3})(Zou *et al*. 2013) and powdered corn cob (0.001 to 0.004 mg cm^{-3}) (Mahmoud 2016), but it is comparable with others such as phosphonated cross-linked polyethylenimine (0.6 to 1.6 mg cm^{-3}) (Saad *et al*. 2015) and orange peels (1.1 to 4.0 mg cm^{-3}) (Mahmoud 2014).

Furthermore, the BDST adsorption capacity, N_o in Table 4 was computed as mg of uranium per cm^3 RSK and in terms of mg of uranium per g of RSK using RSK bulk density of "170 mg cm^{-3}". This allows a direct comparison of column data with equilibrium isotherm data, as shown in Fig. 5 of the normalized isotherm (C_e/C_o *vs*. q_e). Increasing in extent of breakthrough caused increasing in solid phase loading of the column and thus increasing of the calculated equilibrium capacity. In contrast, with increasing value of the % breakthrough, the value of equilibrium adsorption based on the isotherm analysis attains a constant value, as shown in Fig. 6. This phenomenon is due to short contact time of uranium with RSK (60 min), and increased breakthrough enabled greater time for intraparticle diffusion. These data revealed the effective use of RSK for uranium removal.

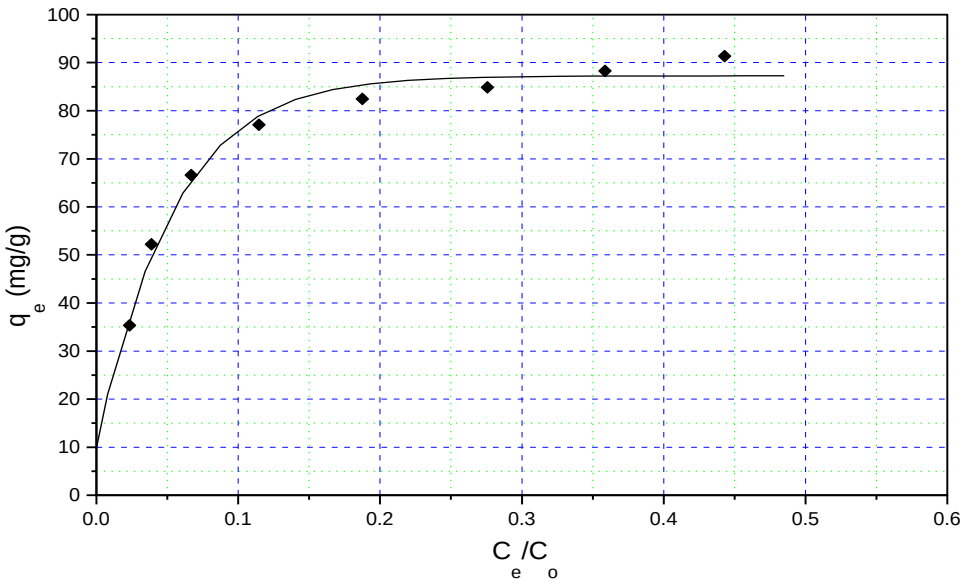

Fig. 5. Normalized (C_e/C_o) equilibrium isotherm of uranium onto RSK carbon. Conditions: time = 60 min, pH 5.5, and v/m= 2000 mL/g

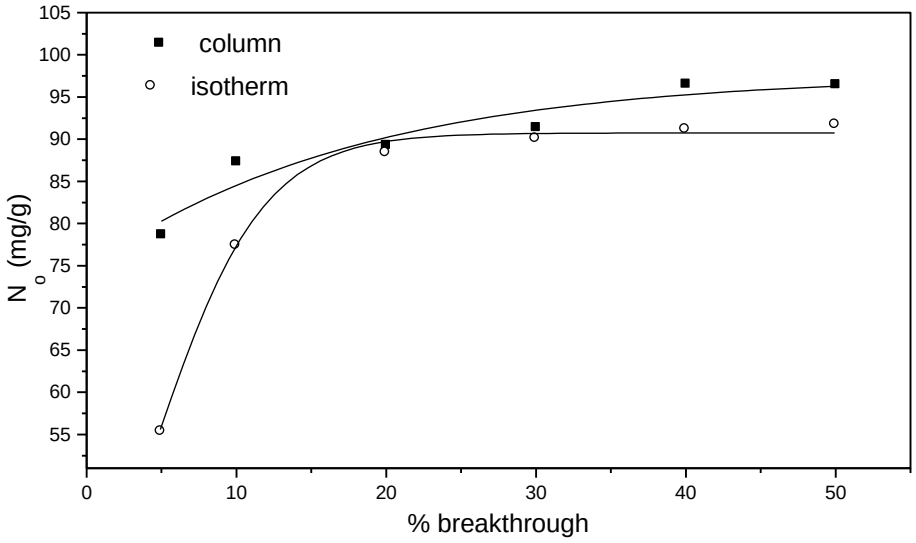

Fig. 6. Comparison of BDST and equilibrium isotherm capacity

The general observation from Fig. 6 is that a small increase in output is attained by changing breakthrough percentage. This is because breakthrough curves are rather steep, so the mass transfer zone become shorter (Magdy and Daifullah 1998). In the BDST model at 50% breakthrough, *i.e.*, $t_b = t_{0.5}$ and $C_o/\underline{C}_b = 0.5$, Eq. 6 is reduced as follows,

$$t_{0.5} = \frac{N_o}{C_o u} L \quad (7)$$

As such, the BDST plot at 50% breakthrough is a straight line that passes through the origin point. This did not happen in the present case even though a linear relationship was obtained (Fig. 7). This non-conformity of the BDST model was in agreement with the literature, and it may be a consequence of there being more than one rate-limiting step in an adsorption process (Sharma and Forster 1995; Zulfadhly *et al*. 2001; Wong *et al*. 2003; Chu and Hashim 2007). The BDST model offers an easy and widespread way to assess sorption-column tests. However, model validity is limited to the range of conditions used (Han *et al.* 2008; Ahmad and Hameed 2010). Sorption rate in immobilized beads is regularly controlled by internal diffusion that is neglected in the BDST model. According to the BDST model, adsorption is controlled by surface chemical reaction between the adsorbent and adsorbate (Lodeiro *et al.* 2006).

It is worth mentioning that theoretical breakthrough curves resulting from the BDST model are symmetric. In this way the breakthrough curve from 0 to 50% breakthrough is of similar shape to the curve from 50 to 100 % breakthrough, which is not true in practice.

Furthermore, a BDST model can be used to estimate the model slope at other flowrates ($Q\backslash$) once the slope (m) at a certain flowrate (Q) is known (Gupta *et al*. 1997; Magdy and Daifullah 1998). The new slope ($m\backslash$) is given by Eq. 8.

$$m\backslash = m\left(\frac{Q}{Q\backslash}\right). \quad (8)$$

Moreover, the BDST model can estimate the bed performance when the initial

concentration, C_o, is changed to a new value, $C\backslash_o$.

The new slope m\ can be written as Eq. 9 (Hutchins 1973), and the new intercept can be written as Eq. 10:

$$m^{\backslash} = m\left(\frac{C_o}{C_o^{\backslash}}\right) \quad (9)$$

$$C_x^{\backslash} = C_x \frac{C_o}{C_o^{\backslash}}\left(\frac{\ln\left(\frac{C_o^{\backslash}}{C_b^{\backslash}} - 1\right)}{\ln\left(\frac{C_o}{C_b} - 1\right)}\right). \quad (10)$$

The prediction efficiency of the BDST analysis was evaluated for uranium adsorption onto RSK column at 50% breakthrough. The BDST equation was applied at flow rate 3 mL/min and used to predict the slope and intercept of BDST equation at the higher flow rate 5 mL/min. The experimental and predicted BDST curves were similar, as shown in Fig. 7, and give good conformity at 100 mg/L of uranium inlet concentration. The BDST results (slope and intercept) for prediction of 200 mg/L are shown in Fig. 8.

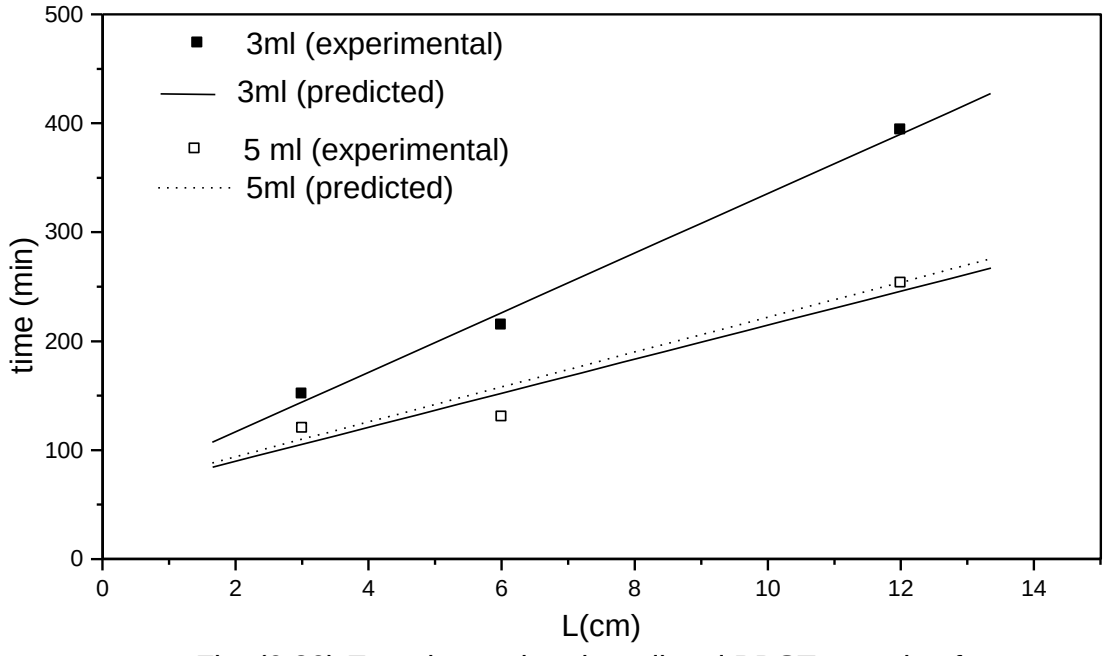

Fig. 7. Experimental and predicted BDST equation for adsorption of uranium at different flow rates

The BDST constants (slope, intercept, and N_o) for the experimental and predicted curve are shown tabulated in Table 5. The calculated BDST slopes were in good agreement with the experimental one, while the values of their intercept slightly varied within a certain limit of experimental error. These results indicate the validity of BDST model for designing of fixed bed adsorption column of uranium onto RSK carbon. The advantage of this procedure is that laboratory tests can provide reliable information without running a pilot test in a large column.

Figure 6 shows that the 50% breakthrough adsorption capacity (N_o) decreases with increasing solution flowrates parallel to values in Table 4. This suggests that to attain longer service times and consequently, higher uptake in a column, lower flow rates should

be used. This is not the same when initial concentration of uranium increases from 100 to 200 mg/L the adsorption capacity almost the same (15×10^3 and 14.8×10^3 mg/cm^3). This phenomenon is due to the high driving force provided by the high concentration, which is reflected by high adsorption capacity.

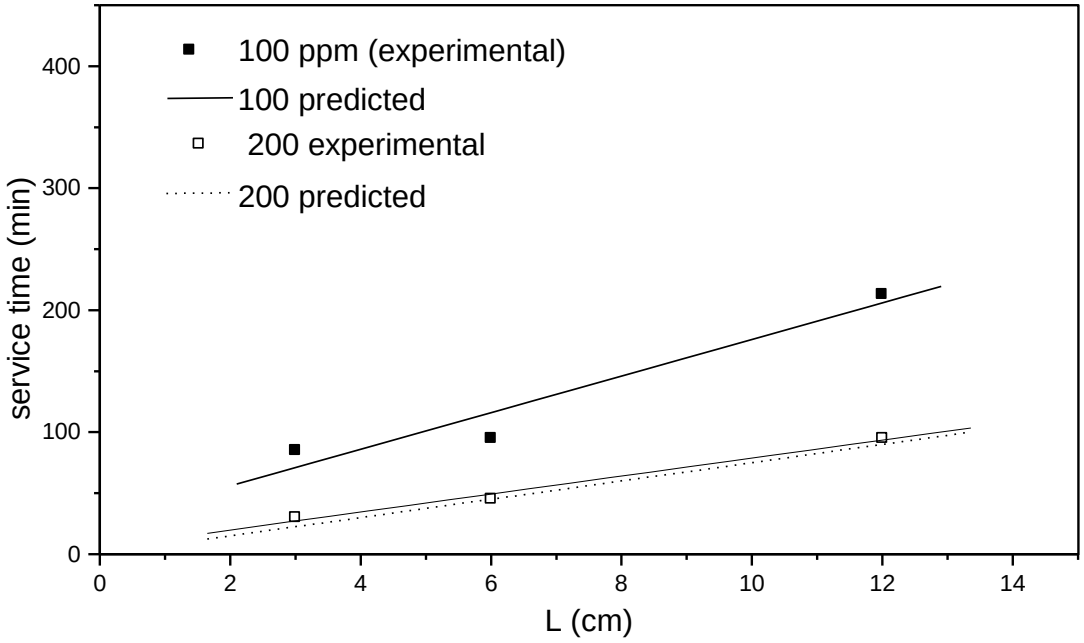

Fig. 8. Experimental and predicted BDST equation for adsorption of uranium at different initial concentration

Table 5. Experimental and Calculated BDST Constants of Uranium Adsorption

Q mL/min	C_o mg/L	Slope		Intercept		N_o *mg cm^{-3} x 10^3*
		Exp.	Calc.	Exp.	Calc.	
3	100	27.3	-	62.1	-	*16.405*
5	100	15	16.2	26	62.1	15.0
5	200	7.4	7.5	0	5	14.8

CONCLUSIONS

1. This investigation showed that KOH-oxidized rice straw-based carbon was an efficient and promising adsorbent for uranium removal from aqueous solutions by means of continuous fixed-bed column.
2. Column performance was dependent on the bed height and adsorbed uranium quantity decreased with increasing bed depth.
3. The BDST models were applied for analysis of experimental data. The calculated BDST slopes were in good agreement with the experimental one, while the values of their intercept slightly varied in certain limit of experimental error.
4. Failure of $t_{0.5}$ *vs.* L plot to pass through the origin indicates that uranium adsorption on RSK carbon involves a complex mechanism with more than one rate-limiting step.

5. These results indicate the validity of BDST model for designing of fixed bed adsorption column of uranium onto RSK carbon.

ACKNOWLEDGMENTS

The authors extend their appreciation to the Deanship of Scientific Research at King Saud University for funding this work through research group No (RG-1436-026).

Competing Interests

The authors declare that they have no competing interests.

REFERENCES CITED

Ahmad, A. A., and Hameed, B. H. (2010). "Fixed-bed adsorption of reactive azo dye onto granular activated carbon prepared from waste," *Journal of Hazardous Materials* 175(1-3), 298-303. DOI: 10.1016/j.jhazmat.2009.10.003

ASTM D6586-00 (2000). "Standard practice for the prediction of contaminant adsorption on GAC in aqueous system using rapid small-scale column tests," ASTM International, West Conshohocken, USA.

Allen, H. E., Chen, Y.-T., Li, Y., Huang, C. P., and Sanders, P. F. (1995). "Soil partition coefficients for Cd by column desorption and comparison to batch adsorption measurement," *Environmental Science & Technology* 29(8), 1887-1891. DOI: 10.1021/es00008a004

Atar, N., Olgun, A., and Wang, S. (2012). "Adsorption of cadmium (II) and zinc (II) on boron enrichment process waste in aqueous solutions: Batch and fixed-bed system studies," *Chemical Engineering Journal* 192, 1-7. DOI: 10.1016/j.cej.2012.03.067

Bohart, G. S., and Adams, E. Q. (1920). "Some aspects of the behavior of charcoal with respect to chlorine," *Journal of the American Chemical Society* 42, 523-544. DOI: 10.1021/ja01448a018

Chang, T. W., and Wang, M. K. (2002). "Assessment of sorbent/water ratio effect on adsorption using dimensional analysis and batch experiments," *Chemosphere* 48(4), 419-426. DOI: 10.1016/S0045-6535(02)00053-X

Chatterjee, A., and Schiewer, S. (2014). "Multi-resistance kinetic models for biosorption of Cd by raw and immobilized citrus peels in batch and packed-bed columns," *Chemical Engineering Journal* 244, 105-116. DOI: 10.1016/j.cej.2013.12.017

Chern, J.-M., and Chien, Y.-W. (2002). "Adsorption of nitrophenol onto activated carbon, isotherms and breakthrough curves," *Water Research* 36(3), 647-655. DOI:10.1016/S0043-1354(01)00258-5

Chu, K. H., and Hashim, M. A. (2007). "Copper biosorption on immobilized seaweed biomass: column breakthrough characteristics," *Journal of Environmental Sciences* 19(8), 928-932. DOI: 10.1016/S1001-0742(07)60153-3

Cortés-Martínez, R., Olguín, M. T., and Solache-Ríos, M. (2010). "Cesium sorption by clinoptilolite-rich tuffs in batch and fixed-bed systems," *Desalination* 258(1), 164-170. DOI: 10.1016/j.desal.2010.03.019

El-Kamash, A. M. (2008). "Evaluation of zeolite A for the sorptive removal of Cs^+ and

Sr^{2+} ions from aqueous solutions using batch and fixed bed column operations," *Journal of Hazardous Materials* 151(2), 432-445. DOI:10.1016/j.jhazmat.2007.06.009

Faust, S. D., and Aly, O. M. (1983). *Chemistry of Water Treatment*, Butterworth, Oxford, UK.

Gupta, V. K., Rastogi, A. Dwivedi, M. K., and Mohan, D. (1997). "Process development for the removal of zinc and cadmium from wastewater using slag—A blast furnace waste material," *Separation Science and Technology* 32(17), 2883-2912. DOI:10.1080/01496399708002227

Han, R., Ding, D., Xu, Y., Zou, W., Wang, Y., Li, Y., and Zou, L. (2008). "Use of rice husk for the adsorption of Congo red from aqueous solution in column mode," *Bioresource Technology* 99(8), 2938-2946. DOI: 10.1016/j.biortech.2007.06.027

Hemming, C. H., Bunde, R. L. Liszewski, M. J. Rosentreter, J. J., and Welhan, J. (1997). "Effect of experimental technique on the determination of strontium distribution coefficients of a surficial sediment from the Idaho National Engineering Laboratory, Idaho," *Water Research* 31(7), 1629-1636. DOI: 10.1016/S0043-1354(96)00408-3

Hussin, L. M. S. (2003). "Treatment of organic-heavy metal waste water using locally available materials," ZagazigUniversity, Zagazig, Egypt.

Hutchins, R. A. (1973). "New simplified design of activated carbon system," *American Journal of Chemical Engineering* 80, 133-138.

Ismaiel, A. A., Aroua, M. K., and Yusoff, R. (2013). "Palm shell activated carbon impregnated with task-specific ionic-liquids as a novel adsorbent for the removal of mercury from contaminated water," *Chemical Engineering Journal* 225, 306-314. DOI: 10.1016/j.cej.2013.03.082

Lodeiro, P., Herrero, R., and de Vicente, M. E. S. (2006). "The use of protonated Sargassum muticum as biosorbent for cadmium removal in a fixed-bed column" *Journal of Hazardous Materials* 137(1) 244-253. DOI: 10.1016/j.jhazmat.2006.01.061

Magdy, Y. H., and Daifullah, A. A. M. (1998). "Adsorption of a basic dye from aqueous solutions onto sugar-industry-mud in two modes of operations," *Waste Management* 18(4), 219-226. DOI: 10.1016/S0956-053X(98)00022-1

Mahmoud, M. A. (2014). "Evaluation of uranium removal from aqueous solution using orange peels in the fixed bed system," *Journal of Chemical Engineering & Process Technology* 5(5), 1-5. DOI: 10.4172/2157-7048.1000200

Mahmoud, M. A. (2016). "Kinetics studies of uranium sorption by powdered corn cob in batch and fixed bed system," *Journal of Advanced Research* 7(1), 79-87. DOI: 10.1016/j.jare.2015.02.004

Marczenko, Z. (1986). *Spectrophotometric Determination of Elements*. New York, John Wiley and Sons Inc.

Muhamad, H., Doan, H., and Lohi, A. (2010). "Batch and continuous fixed-bed column biosorption of Cd^{2+} and Cu^{2+}," *Chemical Engineering Journal* 158(3), 369-377. DOI: 10.1016/j.cej.2009.12.042

Porro, I., Newman, M. E., and Dunnivant, F. M. (2000). "Comparison of batch and column methods for determining strontium distribution coefficients for unsaturated transport in basalt," *Environmental Science & Technology* 34(9), 1679-1686. DOI: 10.1021/es9901361

Rojas-Mayorga, C. K., Bonilla-Petriciolet, A. Sánchez-Ruiz, F. J. Moreno-Pérez, J.

Reynel-Ávila, H. E. Aguayo-Villarreal, I. A., and Mendoza-Castillo, D. I. (2015). "Breakthrough curve modeling of liquid-phase adsorption of fluoride ions on aluminum-doped bone char using micro-columns, Effectiveness of data fitting approaches," *Journal of Molecular Liquids* 208, 114-121. DOI: 10.1016/j.molliq.2015.04.045

Saad, D. M., Cukrowska, E., and Tutu, H. (2015). "Column adsorption studies for the removal of U by phosphonated cross-linked polyethylenimine, modelling and optimization," *Applied Water Science* 5(1), 57-63. DOI: 10.1007/s13201-014-0162-1

Salem, N. A., and Yakoot, S. M. (2017). "Equilibrium and thermodynamics for adsorption of uranium onto potassium hydroxide oxidized carbon," *Desalination and Water Treatment* 72(4), 335-342. DOI: 10.5004/dwt.2017.20448

Setshedi, K. Z., Bhaumik, M. Onyango, M. S., and Maity, A. (2015). "High-performance towards Cr(VI) removal using multi-active sites of polypyrrole–graphene oxide nanocomposites, Batch and column studies," *Chemical Engineering Journal* 262, 921-931. DOI: 10.1016/j.cej.2014.10.034

Shahbazi, A., Younesi, H., and Badiei, A. (2011). "Functionalized SBA-15 mesoporous silica by melamine-based dendrimer amines for adsorptive characteristics of Pb(II), Cu(II) and Cd(II) heavy metal ions in batch and fixed bed column," *Chemical Engineering Journal* 168(2), 505-518. DOI: 10.1016/j.cej.2010.11.053

Sharma, D. C., and Forster, C. F. (1995). "Column studies into the adsorption of chromium (VI) using sphagnum moss peat," *Bioresource Technology* 52(3), 261-267. DOI: 10.1016/0960-8524(95)00035-D

Tan, W. T., Lee, C. K., and Ng, K. L. (1996). "Column studies of copper(II) and nickel(II) ions sorption on palm pressed fibres," *Environmental Technology* 17(6), 621-628. DOI: 10.1080/09593331708616426

Tofan, L., Teodosiu, C. Paduraru, C., and Wenkert, R. (2013). "Cobalt (II) removal from aqueous solutions by natural hemp fibers. Batch and fixed-bed column studies," *Applied Surface Science* 285, 33-39. DOI: 10.1016/j.apsusc.2013.06.151

U.S. Army Corps of Engineers (USACE) (2001). *Engineering and Design: Adsorption Design Guide*, Washington, D.C.

Vijayaraghavan, K., Jegan, J. Palanivelu, K., and Velan, M. (2005). "Biosorption of cobalt(II) and nickel(II) by seaweeds, batch and column studies," *Separation and Purification Technology* 44(1), 53-59. DOI: 10.1016/j.seppur.2004.12.003

Walker, G. M., and Weatherley, L. R. (2001). "COD removal from textile industry effluent, pilot plant studies," *Chemical Engineering Journal* 84(2), 125-131. DOI: 10.1016/S1385-8947(01)00197-8

Wise, W. R. (1993). "Effects of laboratory-scale variability upon batch and column determinations of nonlinearly sorptive behavior in porous media," *Water Resources Research* 29(9), 2983-2992. Doi: 10.1029/93WR00967

Wong, K. K., Lee, C. K. Low, K. S., and Haron, M. J. (2003). "Removal of Cu and Pb from electroplating wastewater using tartaric acid modified rice husk," *Process Biochemistry* 39(4), 437-445. DOI: 10.1016/S0032-9592(03)00094-3

Xu, Z., Cai, J.-g. and Pan, B.-c. (2013). "Mathematically modeling fixed-bed adsorption in aqueous systems," *Journal of Zhejiang University Science* A 14(3), 155-176. DOI: 10.1631/jzus.A1300029

Yakout, S. M. (2015). "Monitoring the changes of chemical properties of rice straw–derived biochars modified by different oxidizing agents and their adsorptive performance for organics," *Bioremediation Journal* 19(2), 171-182. DOI:

10.1080/10889868.2015.1029115
Yakout, S. M. (2016). "Effect of porosity and surface chemistry on the adsorption-desorption of uranium(VI) from aqueous solution and groundwater," *Journal of Radioanalytical and Nuclear Chemistry* 308(2), 555-565. DOI: 10.1007/s10967-015-4408-7
Yakout, S. M., Daifullah, A. M., and El-Reefy, S. A. (2015). "Pore structure characterization of chemically modified biochar derived from rice straw," *Environmental Engineering and Management Journal* 14(2), 473-480.
Yakout, S. M., Metwally, S. S., and El-Zakla, T. (2013). "Uranium sorption onto activated carbon prepared from rice straw. Competition with humic acids," *Applied Surface Science* 280, 745-750. DOI: 10.1016/j.apsusc.2013.05.055
Yakout, S. M., and Rizk, M. A. (2015). "Adsorption of uranium by low-cost adsorbent derived from agricultural wastes in multi-component system," *Desalination and Water Treatment* 53(7), 1917-1922. DOI:10.1080/19443994.2013.860625
Yan, Y., An, Q. Xiao, Z. Zheng, W., and Zhai, S. (2017). "Flexible core-shell/bead-like alginate@PEI with exceptional adsorption capacity, recycling performance toward batch and column sorption of Cr(VI)," *Chemical Engineering Journal* 313, 475-486. DOI: 10.1016/j.cej.2016.12.099
Yang, X., Shi, Z., and Liu, L. (2015). "Adsorption of Sb(III) from aqueous solution by QFGO particles in batch and fixed-bed systems," *Chemical Engineering Journal* 260, 444-453. DOI: 10.1016/j.cej.2014.09.036
Zou, W., Zhao, L., and Zhu, L. (2013). "Adsorption of uranium(VI) by grapefruit peel in a fixed-bed column, experiments and prediction of breakthrough curves," *Journal of Radioanalytical and Nuclear Chemistry* 295(1), 717-727. DOI: 10.100

Article submitted: July 10, 2018; Peer review completed: September 17, 2018; Revised version received: September 27, 2018; Accepted: September 28, 2018; Published: October 31, 2018.
DOI: 10.15376/biores.13.4.9143-9157